Morphology of Blends of Linear and Short-Chain Branched Polyethylenes in the Solid State by Small-Angle Neutron and X-ray Scattering, Differential Scanning Calorimetry, and Transmission Electron Microscopy

G. D. Wignall,*,† R. G. Alamo,*,‡ J. D. Londono,†,§ L. Mandelkern,|| M. H. Kim,‡,⊥ J. S. Lin,† and G. M. Brown#

Solid State Division, Oak Ridge National Laboratory,▽ Oak Ridge, Tennessee 37831-6393; Department of Chemical Engineering, College of Engineering, Florida Agricultural and Mechanical University and Florida State University, Tallahassee, Florida 32310; Institute of Molecular Biophysics, Florida State University, Tallahassee, Florida 32306; Baytown Polymers Center, EXXON Chemical Company, Baytown, Texas 77522

Received July 30, 1999; Revised Manuscript Received October 19, 1999

ABSTRACT: Differential scanning calorimetry (DSC), transmission electron microscopy (TEM), and small-angle neutron and X-ray scattering (SANS and SAXS, respectively) have been used to investigate the solid-state morphology of blends of linear (high-density) and model short-chain branched (linear-low-density) polyethylenes (HDPE/LLDPE). SANS indicates that the mixtures are homogeneous in the melt for all compositions when the ethyl branch content in the copolymer is low (i.e., <4 branches/100 backbone carbon atoms for a molecular weight of $M_w \sim 10^5$). However, due to the structural and melting point differences between HDPE and LLDPE, the components may phase segregate in the solid state. The degree of separation is therefore controlled by the crystallization kinetics. DSC, TEM, SAXS, and SANS experiments have been used to investigate the solid-state morphology as a function of component composition, the thermal history, and the rate of cooling. It is shown that the combination of scattering, microscopy, and calorimetric techniques can provide detailed insight into the compositions of the various populations of the lamellar crystals and the amorphous regions that surround them.

Introduction

The melting temperatures of different polyethylenes depend on both the molecular constitution and crystallization conditions. High-density polyethylene (HDPE), with a peak melting point range $130 < T_m < 135$ °C, is the more highly crystalline form because it is essentially devoid of branching. Low-density polyethylene (LDPE), with a melting temperature typically $108 < T_m < 115$ °C, contains some short-chain branches as well as a few long-chain branches. Linear-low-density polyethylene (LLDPE) has a more homogeneous side branch length, typically with no long-chain branches. The properties of the individual species can be altered by mixing the components, and blends of HDPE, LDPE and LLDPE are widely used commercially. However, understanding of the mechanical and melt flow properties of such blends is handicapped by the absence of a consensus concerning the miscibility of the components, both in the melt and solid states. We have previously used SANS to investigate the melt-miscibility of both HDPE/LDPE and HDPE/LLDPE polyethylenes, and the results[1−3] confirm that the mixtures are homogeneous in the melt for all compositions when the branch content is low (i.e., <4 branches/100 backbone carbon atoms for a molecular weight of $M_w \sim 10^5$ g/mol). However, when the branch content is higher (typically ≥8 branches/100 backbone carbons), the blends phase separate in the melt.

Crist and co-workers[4] have also used SANS to determine the phase behavior of 50/50 blends of HDPE and hydrogenated polybutadienes (HPBD) that are structurally analogous to ethylene−butene-based LLDPE although the former have narrower molecular weight and composition distributions than those of the LLDPE (metallocene or Ziegler). The study carried out by Crist also indicated that the blends are homogeneous in the melt when the branch content is low.

The objective of this work is to use the complementary information given by DSC, TEM, SANS, and SAXS to establish the morphology of HDPE/LLDPE blends that arise on cooling of a homogeneous melt. Blends crystallized isothermally or under rapid or slow processes are studied. To our knowledge, this is the first report that analyzes solid polyethylene blends using four different techniques. Other studies of similar blends have been carried out with more heterogeneous samples using just one or two of these techniques.[5−11] To minimize effects on the morphology due to broad molecular weight or branching composition distributions,[12] a hydrogenated polybutadiene was chosen as the LLDPE model compound. A study of the cocrystallization behavior of the same protonated blends has been reported.[13] The cocrystallization was studied by DSC and solvent extraction procedures. A high degree of cocrystallization was found in the rapidly crystallized mixtures, whereas segregated crystals were formed after isothermal crystal-

† Oak Ridge National Laboratory.
‡ College of Engineering, Florida Agricultural and Mechanical University and Florida State University.
§ Current address: DuPont Central Research and Development Experimental Station, Building E323, P.O. Box 80323.
|| Institute of Molecular Biophysics, Florida State University.
⊥ Current address: Chemical and Analytical Sciences Division, Oak Ridge National Laboratory, Oak Ridge, TN 37831.
EXXON Chemical Company.
▽ Managed by Lockheed Martin Energy Research Corporation under Contract DE-AC05-84OR2140 for the U. S. Department of Energy.

10.1021/ma9912655 CCC: $19.00
Published on Web 01/04/2000

Table 1. Molecular Weights, Polydispersity and Branch Content of Homopolymer Components of Blends

homopolymer	$10^{-3}\ M_w$	M_w/M_n	ethyl branches per 100 backbone carbons
d-HDPE	104.6[a]	5.6	0
HPBD-2[b]	108.0	1.3	2.2

[a] For d-HDPE, the M_w was calculated as if it contained H atoms rather than D atoms. [b] Hydrogenated polybutadiene was used as model linear-low-density polyethylene.

lization, as indicated by the ability to extract quantitatively the pure copolymer at its dissolution temperature.

In addition to the composition of each component in the crystalline phase(s) given by DSC, SANS is used in this work to establish the composition of the amorphous region(s) surrounding the crystals. SAXS and TEM are used as complementary techniques to determine the lamellar structure.

Experimental Section

Blend Preparation. The molecular weights, polydispersities, and branch contents of the two components are listed in Table 1. d-HDPE is a deuterated linear polyethylene purchased from Isotec, Inc. The hydrogenated polybutadiene (HPBD-2) was purchased from the Phillips Co. Its structure is identical to a random ethylene-1-butene copolymer. It has very narrow molecular weight and composition distributions and, thus, serves as a model component of linear-low-density polyethylenes (LLDPE). As seen in Table 1, the level of branching is low (2.2 mol %), such that all blends are homogeneous in the melt, as demonstrated by SANS.[1]

The mixtures were prepared by dissolving the appropriate percentages by mass (total weight ~ 300 mg) in 125 mL of *o*-dichlorobenzene at 178 °C and stirring for 15 min. The solution was then rapidly quenched into 2.2 L of chilled methanol (~60 °C). The crystallites in the solution were decanted, filtered, and dried in a vacuum oven at 60 °C. Disks ~1 mm thick were obtained by compression molding the crystallites at 190 °C (~10 min) followed by crystallization. The mass-based compositions of the d-HDPE/HPBD-2 blends are 20/80, 50/50, and 80/20. The morphology of the solid blends was changed by varying the crystallization procedures. Rapidly quenched blends were obtained by quickly quenching the molten disks into a dry ice/2-propanol saturated mixture (−78 °C). The slowly cooled blends were prepared by cooling the melt (190 °C) at 0.8 °C/min to room temperature. A set of samples were also prepared by isothermal crystallization at 117 °C. In the two latter preparations, the disks were placed in evacuated glass tubes. The isothermal crystallizations were carried out for 18 h in a silicon oil bath with temperature controlled to ±0.1 °C. After this time elapsed, the tubes were taken from the bath to room temperature.

DSC and TEM Characterization. The melting behavior was studied by differential scanning calorimetry using Perkin-Elmer models DSC-2B or DSC-7. Both instruments were calibrated using indium as standard. Melting endotherms were obtained at 10 °C/min in 2−3 mg of sample. The degrees of crystallinity were calculated from the heat of fusion using 289 J/g as the heat of fusion of 100% crystalline-protonated polyethylene[14] and 255 J/g for the heat of fusion of the deuterated pure crystal.[15,16]

Samples to be analyzed by TEM were cryosectioned at −130 °C to expose the plane of analysis and stained in the vapors of ruthenium tetroxide for 2.5−3 h.[17] Ultrathin sections were cut at ambient temperature using a water flotation-bath-equipped Reichert-Jung Ultracut E ultramicrotome and diamond knife. The sections were analyzed in a transmission electron microscope (Philips EM-300 at 100 kV accelerating voltage or JEOL 2000FX at 160 kV). It has been documented that the staining technique is a much better method than permanganic etching to reveal detailed morphological features of the lamellae.[18]

Small-Angle Neutron and X-ray Scattering. The SANS data were collected at room temperature on the W. C. Koehler 30 m facility[19] at the Oak Ridge National Laboratory (ORNL) via a 64 × 64 cm^2 area detector with cell (element) size ~ 1 cm^2 and a neutron wavelength, $\lambda = 4.75$ Å. The detector was placed at sample−detector distances in the range 14−19 m, and the data were corrected for instrumental backgrounds and detector efficiency on a cell-by-cell basis, prior to radial (azimuthal) averaging to give a Q range of $0.003 < Q = 4\pi\lambda^{-1} \sin\Theta < 0.04$ Å^{-1}, where 2Θ is the angle of scatter. The sample cross sections were obtained by subtracting the intensities of the corresponding sample cells with quartz windows, which formed only a minor correction to the data.

The net intensities were converted to an absolute (±3%) differential cross section per unit sample volume [$d\Sigma/d\Omega(Q)$ in units of inverse centimeters] by comparison with precalibrated secondary standards,[20] based on the measurement of beam flux, vanadium incoherent cross section, the scattering from water, and other reference materials. The cross sections of fully labeled (d-HDPE) and unlabeled (HPBD-2) linear and branched blanks were also measured as a basis for subtracting the coherent and incoherent backgrounds.[21] The former arises mainly from void scattering and is negligible for $Q > 0.01$ Å^{-1}. The latter is a flat background of ~0.1−0.7 cm^{-1} due to the H^1 incoherent cross section and may be subtracted via empirical methods.[21] The sample transmission was measured as described previously,[1−3] and in practice, it only changed by <1% between 23 and 200 °C, because the increasingly incoherent cross section of H^1 is offset by the decreasing polymer density.

The SAXS experiments were performed on the ORNL 10 m SAXS instrument,[22,23] using Cu Kα radiation ($\lambda = 1.54$ Å) with pinhole collimation and hence minimal instrumental smearing effects.[24] The sample−detector distance was 5.1 m and a 20 × 20 cm^2 area detector was used with cell (element) size ~3 mm. Corrections for instrumental backgrounds and detector efficiency (via an Fe^{55} standard which emits γ-rays isotropically) were made on a cell-by-cell basis, prior to radially averaging in the Q range $0.005 < Q < 0.12$ Å^{-1}, and by converting to an absolute differential cross section by means of precalibrated standards.[25]

For HDPE/LDPE mixtures in the solid state, it has been shown[1] that the formalism proposed by Debye and Bueche[26,27] (DB) was appropriate, with a cross section of the form

$$\frac{d\Sigma}{d\Omega}(Q) = \frac{8\pi a_1^3 \varphi_1 \varphi_2 [\rho_1 - \rho_2]^2}{(1 + Q^2 a_1^2)^2} \qquad (1)$$

where a_1 is a length characterizing the spatial dimensions via an exponential correlation function.[26,27] φ_1 and φ_2 are the volume fractions and ρ_1 and ρ_2 are the scattering length densities of the two phases.[3] Figure 1

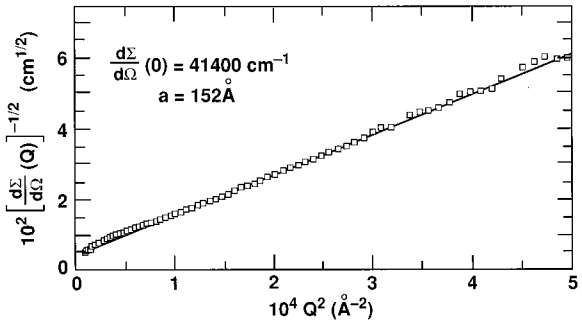

Figure 1. Debye−Bueche plot for 20/80 d-HDPE/HPBD-2 blend isothermally crystallized at 117 °C.

shows a DB plot [$(d\Sigma/d\Omega)^{-0.5}$ vs Q^2] of the SANS data from a 20/80 d-HDPE/HPBD-2 sample crystallized at 117 °C. The DB plot is linear to a good approximation, although there is a hint of a downward deviation at the lowest Q values. A similar phenomenon was observed by Debye and co-workers,[26,27] who introduced a second (Gaussian) correlation function and length (a_2) to characterize larger structural features. When the HDPE/LDPE SANS data were fitted by the 2-correlation function model,[3] the values of a_2 were ∼10^3 Å, and it is probable that similar structures are present in the d-HDPE/HPBD-2 blends that cannot be resolved with pinhole SANS instrumentation. These would need to be studied with ultrahigh-resolution SANS facilities, which are now becoming available.[28] Such dimensions reflect scattering length density fluctuations arising from morphological features on length scales larger than the individual lamellae (with long periods of ∼10^2 Å), which are the primary focus of this research. These domain sizes may be estimated from the mean chord intercept lengths[1,3,26,27]

$$L_1 = a_1/\varphi_1 \tag{2}$$

$$L_2 = a_1/\varphi_2 \tag{3}$$

where the correlation length (a_1) is derived[1,3] from the ratio of slope/intercept of the DB plot. Thus, the mean cord intercept of the lamellae derived from Figure 1 is ∼200 Å, and the integrated area under the curve is the SANS invariant, which for a 2-phase system is given by[29]

$$Q_0 = \int_0^\infty Q^2 d\Sigma/d\Omega(Q)\, dQ = 2\pi^2\varphi_1\varphi_2[\rho_1 - \rho_2]^2 \tag{4}$$

and this provides another parameter that can be extracted from the data to give an independent check on the structural model for the blend morphology.

Results and Discussion

(a) Isothermally Crystallized Blends. The melting endotherms of the blends and pure components crystallized at 117 °C are given in Figure 2. This crystallization temperature was chosen as being well above the melting temperature of the pure HPBD and below the melting of the linear polyethylene. Thus, based on previous kinetic studies,[13,31] a segregation of the components in different lamellar crystallites is expected in these blends, from the difference in crystallization kinetics. We first note from the thermogram of the pure linear component the presence of a small population of crystals (−16% by mass) that melt at ∼116 °C, a temperature lower than that for the crystals formed at 117 °C. These

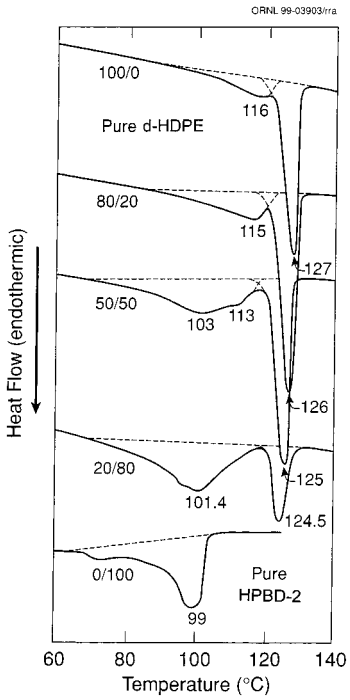

Figure 2. DSC melting endotherms for d-HDPE/HPBD-2 blends isothermally crystallized at 117 °C.

Table 2. Melting Temperatures and Mass Derived Degrees of Crystallinity of d-HDPE/HPBD-2 Blends Isothermally Crystallized at 117 °C

comp. (mass %) d-HDPE/HPBD-2	T_m (°C)		$(1-\lambda)_{\Delta H}$ (%) exptl		$(1-\lambda)_{\Delta H}$ (%)[a] calcd		
0/100	99	71.8	24				24
20/80	124.5	101.4	8.2	22.5	10.5	3.8	19.2
50/50	125.4	113, 103	21.6	20.3	26.2	9.4	12
80/20	126.1	115.3	36.6	16.5	41.8	15.1	5
100/0	126.8	116.2	52.3	18.9	52.3	18.9	

[a] Calculated assuming that both polymers crystallize in separate lamellae.

crystals are formed during the slow-cooling process from 117 °C to room temperature. The HPBD-2 does not crystallize at 117 °C; thus, the endotherm shown in Figure 2 for the pure HPBD-2 corresponds to crystals that were formed during cooling.

The thermograms of the blends show two melting peaks consistent with the formation of separate crystals from both components. From the heat of fusion, the percentage crystallinity *by mass* was obtained for each peak and compared with the expected value in the blends if both components had crystallized independently. These values (based on total mass) and the melting temperatures are given in Table 2. The calculated values for the degrees of crystallinity list a separate component of d-HDPE crystals formed on cooling. This fraction varies from 3.8% for the 20/80 mixture to 15.1% in the 80/20. When this quantity is added to the calculated mass percentage of crystals formed from the branched component (HPBD-2), the resulting value agrees closely with the experimental degree of crystallinity obtained from the low-temperature endotherm of Figure 2.

The agreement between the degree of crystallinity from the heat of fusion of the high-temperature endotherm and that calculated based on the pure linear endotherm crystallized at 117 °C is also good. This fact and the clear double melting found for the blends allows

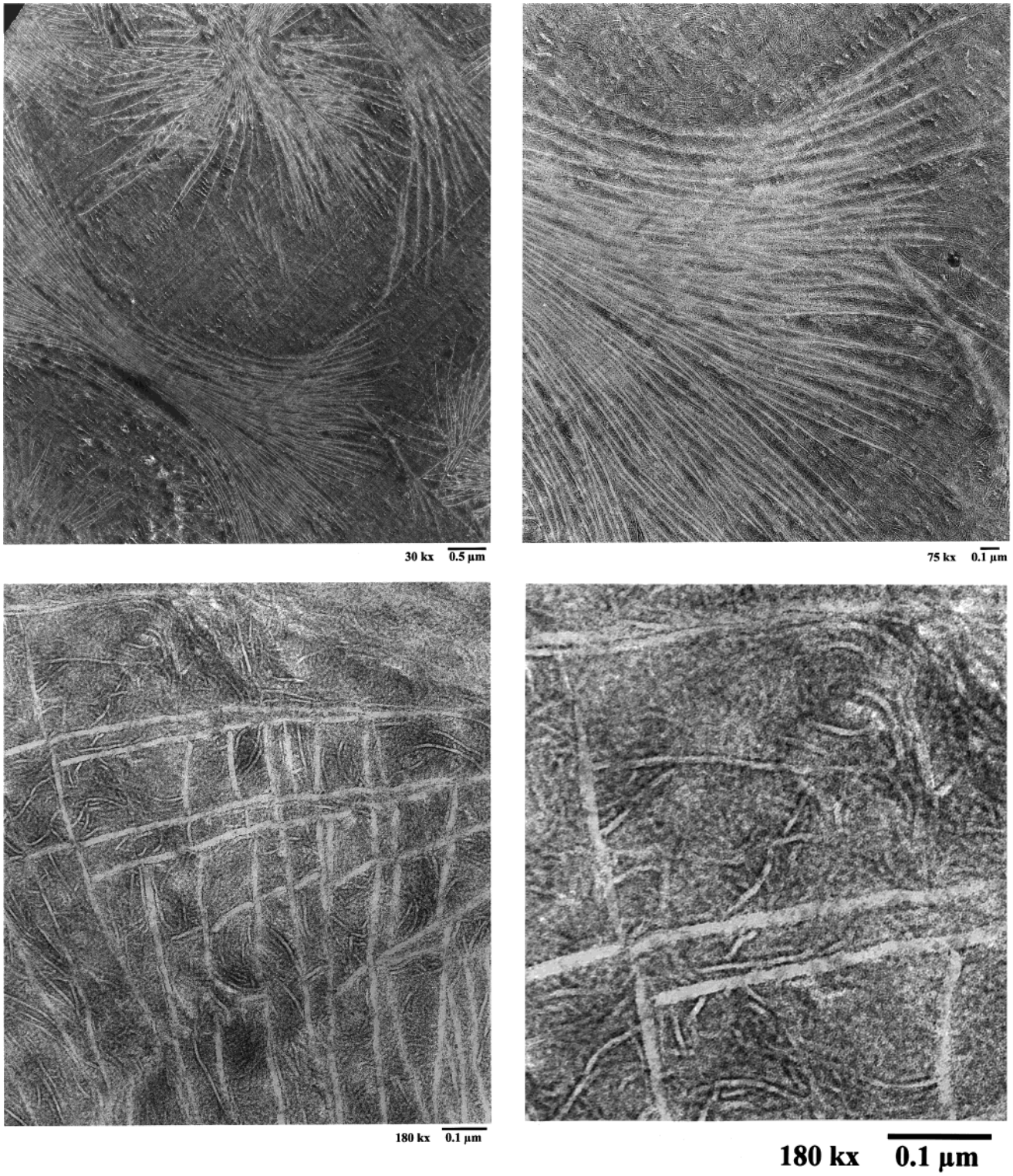

Figure 3. (a) TEM of d-HDPE/HPBD-2 (50/50) blend isothermally crystallized at 117 °C. (b), (c), and (d) Enlarged sections of the same blend.

us to conclude that during isothermal crystallization at 117 °C only crystals from the linear component are formed. The question that arises is whether there is cocrystallization of both types of molecules in the crystals formed on slow cooling after the isothermal crystallization is halted. The study of the melting behavior of the blends by DSC by itself cannot address this issue. Even if the crystals formed from the linear component on cooling crystallized separately from the branched component, their melting peaks overlap in a broad range of temperatures, making a distinction between them impossible. In this respect, the broad double peak low-temperature endotherm seen in Figure 1 for the 50/50 mixture seems to indicate that, in fact, a double population of crystals is formed on cooling. As we shall see later, SANS will help to resolve this issue and will allow us to determine the morphology of the amorphous phase surrounding these crystals.

To corroborate the initial conclusions made from the melting behavior, thin sections of these isothermally crystallized blends were cut and stained, and the crystalline morphology was resolved by transmission

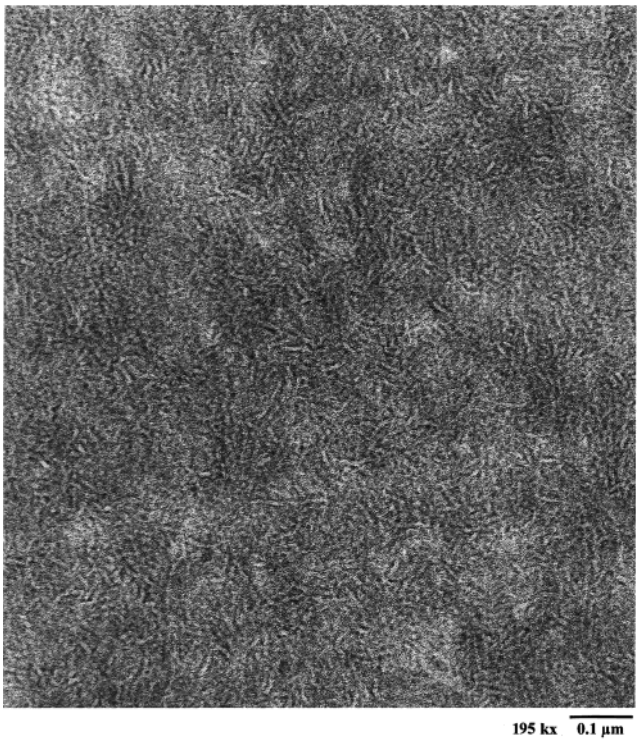

Figure 4. TEM of HPBD-2 rapidly quenched.

electron microscopy. Micrographs of the 50/50 blend are shown in Figure 3. Parts b, c, and d of Figure 3 are magnified areas of the same blend. Well-organized interpenetrating wheat sheaves, formed in the process of crystallization at high temperature of the linear component, contrast in a background of thinner and more poorly formed lamellae. The average thickness of the thick lamellae is 170 Å, and the thin lamellae range from 60 to 80 Å thick. The highest temperature endotherm corresponds to the melting of the thicker d-HDPE lamellae. The morphological details of the thin lamellae that fill the interlamellar spaces within the wheat sheaves and comprise the semicrystalline matrix become clearer in the magnified sections shown in parts b and c of Figure 3. Two types of lamellae of similar thickness form the background; one population of thin lamellae is better defined and has more contrast. The lamellae in this group are straighter than those of the second, more poorly defined population of curved, segmented lamellae.

The morphology of the thin lamellae that comprise the background (in Figure 3b) can be compared with the morphology of the pure branched HPBD-2 component crystallized under the same conditions (in Figure 4). This comparison allows us to clearly identify the poorly formed, twisted, and segmented lamellae of low contrast as crystals formed from the pure branched HPBD-2 component. The thin, straighter lamellae of the matrix and between the HDPE lamellae of the interpenetrating sheaves are cocrystals formed on cooling from the uncrystallized linear and branched polyethylenes, as will be demonstrated by SANS. Figure 3d clearly shows that these two types of thin lamellae reside throughout the system in the interlamellar region and in the matrix between sheaves and were homogeneously distributed (mixed) in the original melt, as previously demonstrated by SANS.[2] These blends, isothermally crystallized or quenched (as we will discuss later), do not show the two types of crystals domains separated on scale of microns that have been attributed to liquid−liquid phase separation in the melt.[18] The number of nucleation events, which controls crystallization kinetics, initiates the growth of the linear component to form sheaves with an open lamellar structure. The branched and uncrystallized linear components crystallize on cooling in the HDPE interlamellar interstices and in the matrix between sheaves.

It has been argued that liquid−liquid phase separation of linear/branched polyethylene blends is concentrated in the branched-rich side of the phase diagram.[8,18] However, our studies by SANS, DSC, and TEM have not found differences in phase behavior with blend composition when the branching content is less than ∼4 mol %. The 20/80 blend (which cystallized at 117 °C) is shown in Figure 5 and represents a compositional region that was claimed to be phase separated in the melt. The general morphological features are very similar to those found for the 50/50 blend. The decreased concentration of the linear component in this blend leads to fewer nucleation sites for the isothermal crystallization of the d-HDPE and to a more open lamellar structure. As seen in Figure 5 and found in the 50/50 blend, well-organized wheat sheaves make up the supermolecular structure of the linear component that crystallizes at 117 °C. The enlarged portion of Figure 5d shows that the wheat sheaf is made of long, well-formed lamellae ∼160 Å thick and a matrix of thin, segmented lamellae that are morphologically similar to the lamellae of the pure branched component shown in Figure 4. In the background are also seen the straighter, thin lamellae that, as mentioned before, can be associated with cocrystals formed from the fraction of linear component that crystallizes on cooling and the longest ethylene sequences of HPBD-2. These lamellae do not seem to be formed by epitaxial crystallization.

In summary, TEM indicates that isothermally crystallized blends contain two main types of lamellae. Thick, long, and well-organized lamellae are formed by the isothermal crystallization of part of the linear component. A second population of thinner lamellae comprises the matrix in which the HDPE wheat sheaves are interspersed. These thinner lamellae correspond to the crystallization, on cooling to room temperature, of the branched polyethylene and the reminder of the linear component. This background matrix may be comprised of lamellae from individual molecules or from cocrystallized ones. Neutron scattering was carried out in these blends to corroborate previous conclusions and distinguish between these two possibilities.

The volume fraction of the crystalline and amorphous contents of each component were calculated from the DSC heats of fusion. The density of the protonated PE crystal was taken as 1 g/cm^3 and that of the amorphous crystal as 0.853 g/cm^3. A 14% difference in the densities of deuterated and protonated polyethylenes was used for amorphous and crystalline samples. The volume-based percentages are listed in Table 3. The fraction of d-HDPE crystals in the blends, formed on cooling, was calculated from the value found in the pure component (18.9% by mass). It varies from 13.4% for the 80/20 blend to 3.2% for the 20/80.

The DB and invariant analyses described in eqs 1−4 are strictly valid only for two-phase systems, whereas the compositions of the various crystals and surrounding amorphous regions (Table 3) indicate that, from a DB formalism, there are more than two phases. For such

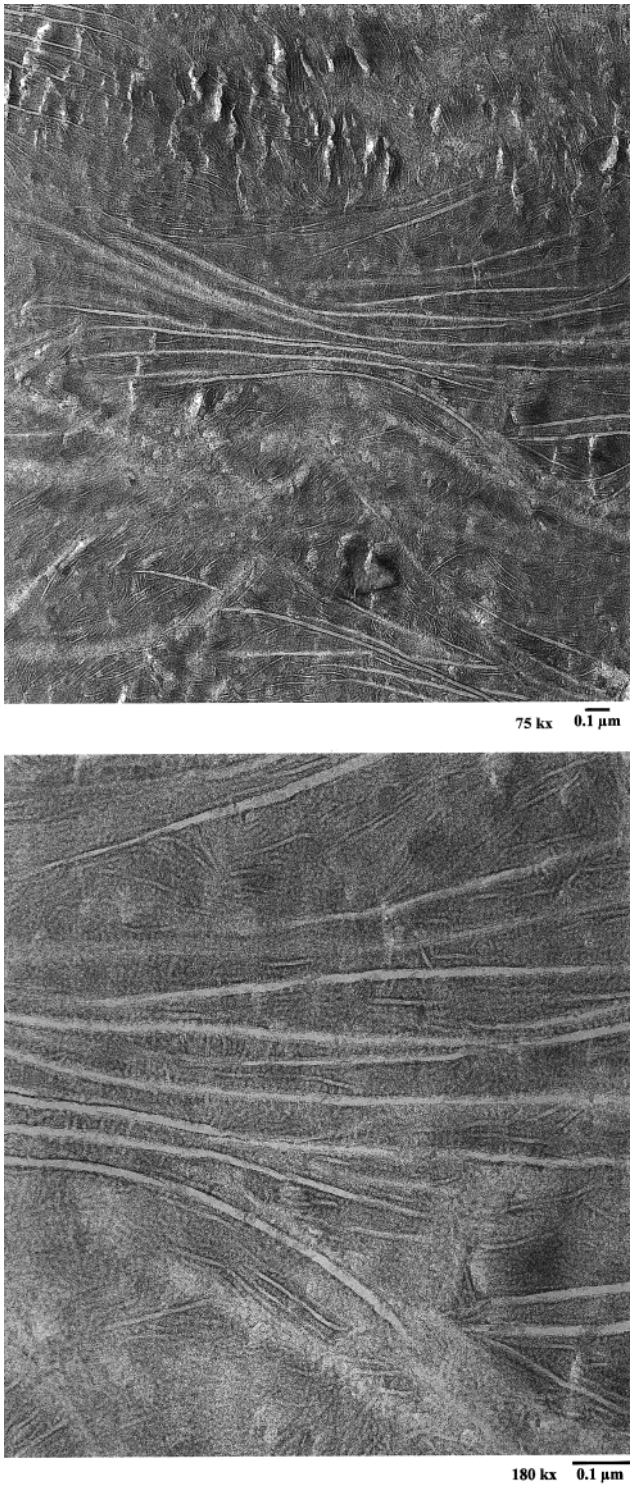

Figure 5. (upper) TEM of d-HDPE/HPBD-2 (20/80) blend isothermally crystallized at 117 °C. (lower) Enlarged section of the same blend.

multiphase systems, an extension of the invariant analysis[29,30] may be employed by generalizing eq 4 and summing over the number of phases involved

$$Q_0 = 2\pi^2 \sum_{i \neq j} \varphi_i \varphi_j [\rho_i - \rho_j]^2 \qquad (5)$$

and such an approach was applied[30] to blends of polycaprolactone and polycarbonate. The ($Q = 0$) cross section [$d\Sigma/d\Omega(0)$] cannot be calculated for multiphase systems, although it may be estimated via a "pseudo-two-phase" model to a good approximation. For example, for the 20/80 sample, the SLD of the HDPE-D crystal is 8.58×10^{10} cm^{-2}, whereas the SLDs of the mixed (HDPE-D/P108) and amorphous crystals are 1.01 and 0.40 ($\times 10^{10}$ cm^{-2}), respectively. Thus, the SANS cross section [$d\Sigma/d\Omega(0)$] can be calculated to a good approximation by grouping the mixed phases into an *average* background ($\rho_{av} = 0.53 \times 10^{10}$ cm^{-2}) surrounding pure HDPE-D crystal in a pseudo-two-phase model. Hence, the invariant was calculated from the multiphase morphology (eq 5), and the ($Q = 0$) cross section was estimated via eq 1 for the pseudo-two-phase model for the two possible morphologies considered above: **(**A) A fraction of the linear component segregates during isothermal crystallization, whereas the remainder cocrystallizes with the branched component on cooling. (B**)** The linear component partially segregates from the branched component during isothermal crystallization. The remainder segregates on cooling. A compositionally mixed homogeneous amorphous phase is assumed to surround the crystals in both cases.

Table 3. Volume-Based Percentage of Components in the Crystalline and Amorphous Regions[a]

comp. d-HDPE/ HPBD-2	crystal[b] d-HDPE	crystal[c] d-HDPE	crystal HPBD-2	amorph. d-HDPE	amorph. HPBD-2
0/100			21.2		78.8
18/82	7.3	3.2	17.6	6.6	65.3
46.7/53.3	20.4	7.7	11.6	17.0	43.3
77.8/22.2	36.1	13.4	5.2	27.0	18.2
100/0	49.8	18.0		32.2	

[a] Blends isothermally crystallized at 117 °C. [b] Fraction formed at 117 °C. [c] Fraction formed on cooling.

To first order, the invariant is calculated for morphology type A as follows:[30]

$$Q_0 = 2\pi^2[\varphi_1\varphi_2(\rho_1 - \rho_2)^2 + \varphi_1\varphi_3(\rho_1 - \rho_3)^2 + \varphi_2\varphi_3(\rho_2 - \rho_3)^2] \qquad (6)$$

where φ is the volume fraction, ρ is the SLD, and the subscripts 1, 2, and 3 denote the mixed amorphous, pure d-HDPE crystals isothermally formed (sheave-like lamellae in Figures 3 and 5), and the mixed background thin crystals formed on cooling, respectively.

Morphology type B adds a fourth component, because the background is assumed to be formed of pure d-HDPE crystals (subscript 3) and pure HPBD-2 crystals (subscript 4). Then, Q_0 for type B was calculated as follows:

$$Q_0 = 2\pi^2[\varphi_1\varphi_2(\rho_1 - \rho_2)^2 + \varphi_1\varphi_3(\rho_1 - \rho_3)^2 + \varphi_1\varphi_4(\rho_1 - \rho_4)^2 + \varphi_2\varphi_3(\rho_2 - \rho_3)^2 + \varphi_2\varphi_4(\rho_2 - \rho_4)^2 + \varphi_3\varphi_4(\rho_3 - \rho_4)^2] \qquad (7)$$

The experimental and calculated Q_0 values are listed in Table 4. As seen in the table, for the 20/80 blend, the calculated Q_0 and the experimental data are identical for morphology type A. Similarly, the value of $d\Sigma/d\Omega(0)$ calculated from the pseudo-two-phase model and eq 1 is, for morphology type A, 38.7×10^3 cm^{-1}, which agrees closely with the experimental value of 41.4×10^3 cm^{-1}. When morphology type B is assumed, the calculated values do not agree with the experimental data for this blend. Thus, SANS confirms that predominantly LLDPE-rich blends crystallize isothermally as two main types of crystals and one mixed amorphous crystal

Table 4. Measured and Calculated Cross Sections and Invariants for d-HDPE/HPBD-2 Blends Isothermally Crystallized at 117 °C from the Melt

comp.[a] d-HDPE/ HPBD-2	corr.[b] length	dΣ/dΩ[c] exptl	Q_0[d] exptl	morph. consid.[e]	dΣ/dΩ[c] calcd[f]	Q_0[d] calcd[f]
18/82	152	41.4	0.009	A	38.7	0.009
				B	57.6	0.013
46.7/53.3	135	59.2	0.018	A	41.1	0.014
				B	62.7	0.021
77.8/22.2	125	36.1	0.0158	A	16.3	0.007
				B	28.3	0.013

[a] Composition in percent volume. [b] Correlation length in angstroms. [c] With $Q = 0$ and in inverse centimeters times 10^{-3}. [d] In inverse centimeters per cubic angstroms. [e] Morphology considered (see text). [f] Calculations assume separation of components as detailed in text.

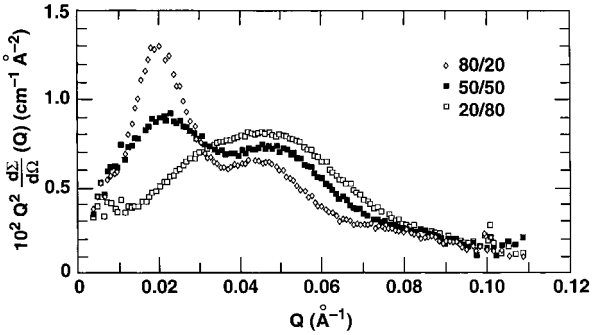

Figure 6. Lorentz-corrected SAXS data for d-HDPE/HPBD-2 blends isothermally crystallized at 117 °C.

surrounding these crystals. One type of crystal is formed from the pure d-HDPE and a second type is formed of mixed-chain crystals (sheaves and background lamellae of Figure 5b).

For the linear-rich, 80/20 blend, the agreement between the experimental and calculated Q_0 and (dΣ/dΩ)(0) values is closer for morphology type B. SANS indicates that for this blend the intensity and invariant conform with a more segregated morphology of the linear and branched components than those for the branched-rich blend. The experimental values for the 50/50 blend lie between the calculated ones. An intermediate morphology between the A and B types is, thus, predicted for the isothermally crystallized 50/50 blends. Part of the linear component that crystallizes on cooling is cocrystallized with the branched HPBD-2, and part crystallizes as pure linear.

In view of the fact that the experiments are independently calibrated with no arbitrary fitting factors in the intensity scale and that the crystal/amorphous compositions are obtained from DSC, the general agreement with the SANS data is excellent. Thus, the two-phase approximation is able to reproduce not only the SANS invariant but also the ($Q = 0$) cross section with good accuracy.

Figure 6 shows the Lorentz-corrected plots (Q^2dΣ/dΩ vs Q) of the absolutely calibrated SAXS data for 80/20, 50/50, and 20/80 wt % HDPE/HPBD samples. Scattering from two different populations of lamellae stacks is clearly seen in the 80/20 and 50/50 blends, with long spacing corresponding to 314 and 140 Å and 289 and 130 Å, respectively. These long periods are calculated from the "peak" positions (Q^*) in Figure 6 as $2\pi/Q^*$ and confirm the two main populations of lamellae with different thicknesses observed by TEM in Figure 3. Only one broad feature is observed for the 20/80 blend, confirming the low content of thick lamellae formed isothermally, as shown in the micrographs of Figure 5. The number of stacks from these thick lamellae is in a much lower concentration than that from the crystals formed on cooling and does not show as a distinct scattering peak. The result is a diffuse scattering from thick to thinner lamellae stacks in a region of Q^* between 0.03 and 0.05 Å^{-1}, which corresponds to long periods between 210 and 125 Å.

Table 5. Percentage Volume of Components in the Crystalline and Amorphous Regions[a]

comp. d-HDPE/ HPBD-2	crystal[b] d-HDPE	crystal[b,c] d-HDPE	crystal[b] HPBD-2	amorph.[b] d-HDPE	amorph.[b] HPBD-2
0/100			22.1		77.9
18/82	8.3	1.85	18.3	7	64.5
46.7/53.3	24.4	3.9	12.2	16.8	42.7
77.8/22.2	40.3	6.1	5.2	30.3	
100/0	47.2	8.5		44.3	

[a] Blends slowly cooled from the melt. [b] In percent. [c] Small population of crystals of lower melting temperature.

Table 6. Measured and Calculated Cross Sections and Invariants for d-HDPE/HPBD-2 Blends Slowly Cooled from the Melt

comp.[a] d-HDPE/ HPBD-2	corr.[b] length	dΣ/dΩ[c] exptl	Q_0[d] exptl	morph. consid.[e]	dΣ/dΩ[c] calcd[f]	Q_0[d] calcd[f]
18/82	91	8.1	0.0071	A	9.6	0.0099
				B	11.9	0.0126
46.7/53.3	80	13.2	0.016	A	10.9	0.017
				B	13.3	0.021
77.8/22.2	75	6.9	0.011	A	4.3	0.008
				B	6.0	0.0124

[a] Composition in percent volume. [b] Correlation length in angstroms. [c] With $Q = 0$ and in inverse centimeters times 10^{-3}. [d] In inverse centimeters per cubic angstroms. [e] Morphology considered (see text). [f] Calculations assume separation of components as detailed in text.

(b) Slowly Cooled Blends. The thermal behavior of these blends is very similar to that shown in Figure 2 for the isothermally crystallized samples. Table 5 gives the DSC-derived compositions (in volume fraction) for the slowly cooled blends. The SANS invariant and cross section were calculated, as for the isothermally crystallized blends with eqs 1 and 5 and are compared with the experimentally determined values in Table 6. The two possible morphologies discussed for the isothermally crystallized blends (A and B types) were also considered.

The data from SANS indicate a similar trend to the morphology of isothermally crystallized blends. For the linear-rich blends, the calculated Q_0 and (dΣ/dΩ)(0) of strongly segregated crystals (morphology type B) agree closely with the experimental SANS intensity ($Q = 0$) and invariant. For the 20/80 blend, the agreement is closer for morphology type A, which assumes some mixing of both types of molecules in the crystals formed in the low-temperature range. The agreement is, nevertheless, not as good as that shown by the samples isothermally crystallized and indicates that some mixing may extend to the crystals formed in the high-temperature region during the slow-cooling process.

The SANS behavior of the 50/50 blends is also very similar to those crystallized at 117 °C (Table 6). The experimentally determined Q_0 value agrees with the

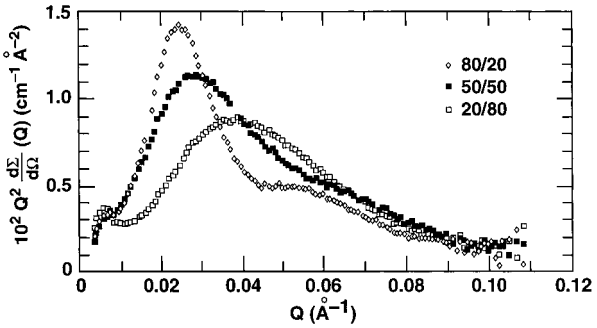

Figure 7. Lorentz-corrected SAXS data for d-HDPE/HPBD-2 blends slowly cooled from the melt.

calculated value for morphology type A, whereas the experimental value for $(d\Sigma/d\Omega)(0)$ is in better agreement with the data calculated for morphology type B. Thus, it is concluded that these 50/50 blends develop a morphology between the A and the B types. The linear crystallizes first in single-component lamellae, and on further cooling, it crystallizes as a pure component and as a cocrystal with part of the branch component.

The strong crystal segregation of the 80/20 slowly cooled blends and the gradual progression toward more mixing in the 50/50 and 20/80 blends are also shown by the SAXS pattern given in Figure 7. The figure shows the Lorentz-corrected plots ($Q^2(d\Sigma/d\Omega)$ vs Q) of the absolutely calibrated SAXS data of the slowly cooled blends. For predominantly linear blends (80/20), two "peaks" or modulations are clearly seen with long spacings of 250 and 118 Å in agreement with the strongly segregated morphology type B. For the predominantly branched samples (20/80), only one feature is observed corresponding to a gradual development of crystals with decreasing thicknesses in the slow-cooling process. The long spacing corresponding to the peak of the Lorentz-corrected plot is 160 Å. The scattering of the 50/50 blends is mainly unimodal (218 Å), with a broad shoulder corresponding to spacings of ~106Å.

(c) Rapidly Quenched Blends. The DSC melting thermograms of the blends and pure components quenched to −78 °C are given in Figure 8. The predominantly linear blends show single melting peaks, whereas much broader endotherms are exhibited by the 50/50 and 20/80 blends. The fact that two melting peaks are not resolved in the thermograms and the monotonic decrease of the melting temperature with increasing concentration of HDBD-2 indicate that the linear and branched polyethylenes cocrystallize when the blends are rapidly quenched from the melt.[13]

The degrees of crystallinity for the quenched pure components and the blends are listed in Table 7, along with the calculated crystallinities based on the compositional amounts of both components. These values are very similar to those obtained from the heat of fusion of the blends and indicate that both components crystallize up to about the same extent as if they were crystallized as a single component. In other words, the cocrystallization in rapidly quenched blends does not reduce significantly the level of crystallinity of both components.

In a series of papers on blends of linear and branched polyethylenes (LDPE and LLDPE were studied as the branched component), it has been argued that the components phase separate in the melt. This interpretation was primarily based on multiple DSC melting peaks displayed by the solid blends, after either quenching or isothermal crystallization from the melt, and the observation from the TEM micrographs of permanganic acid-etched blends containing micron-scale regions with different morphologies (see Morgan et al.[18] and references herein). The branched polyethylenes used in those works are, however, more polydisperse than the model compound HPBD-2 used in the present work.

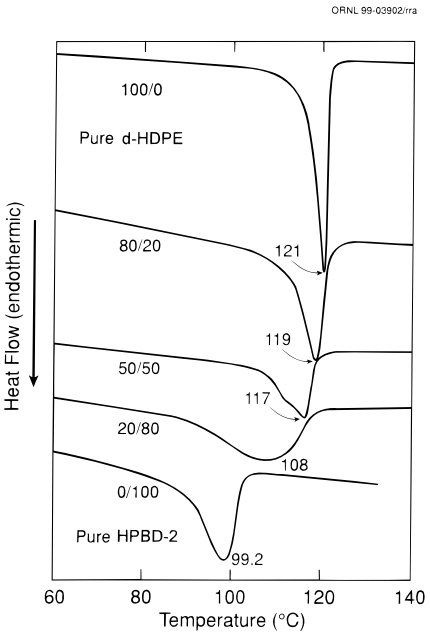

Figure 8. DSC melting endotherms for d-HDPE/HPBD-2 blends rapidly quenched from the melt.

Table 7. Melting Temperatures and Mass Derived Degrees of Crystallinity of d-HDPE/HPBD-2 Blends Rapidly Quenched to −78 °C

comp. (mass %) d-HDPE/HPBD-2	T_m (°C)	$(1-\lambda)_{\Delta H}$ (%) exptl	$(1-\lambda)_{\Delta H}$ (%)[a] calcd
0/100	99.2	21.8	21.8
20/80	107.6 ± 1	22.6	26.0
50/50	117.0	32.0	32.2
80/20	119.0	39.0	38.4
100/0	121	42.6	42.6

[a] Calculated assuming that both polymers crystallize in separate lamellae.

TEM was also carried out on the model blends studied here to determine whether this bimodal morphology was present. As previously indicated,[2,32] the neutron scattering results of these blends in the melt state are consistent with single-phase systems. Moreover, transmission electron micrographs were also obtained from quenched 25/75 blends (Figure 9). This is a composition inside the region that has been claimed to have liquid−liquid phase separation in the melt.[8,18] There was no indication of a bimodal morphology in this micrograph. Upon quenching, the linear and branched components cocrystallize into spherulites comprised of 80 Å thick constituent lamellae and a background of more segmented and curved lamellae about 60 Å thick. It resembles closely the morphology of the region between axialites of the 20/80 blend isothermally crystallized (see parts A and B of Figure 5) that was formed on cooling after the isothermal crystallization was halted. A micrograph of a more extended area shows a homogeneous 2 μm diameter spherulitic morphology. We, thus, conclude that these blends are homogeneous in the melt and that upon quenching the linear component cocrystallizes predominantly with long sequences of the

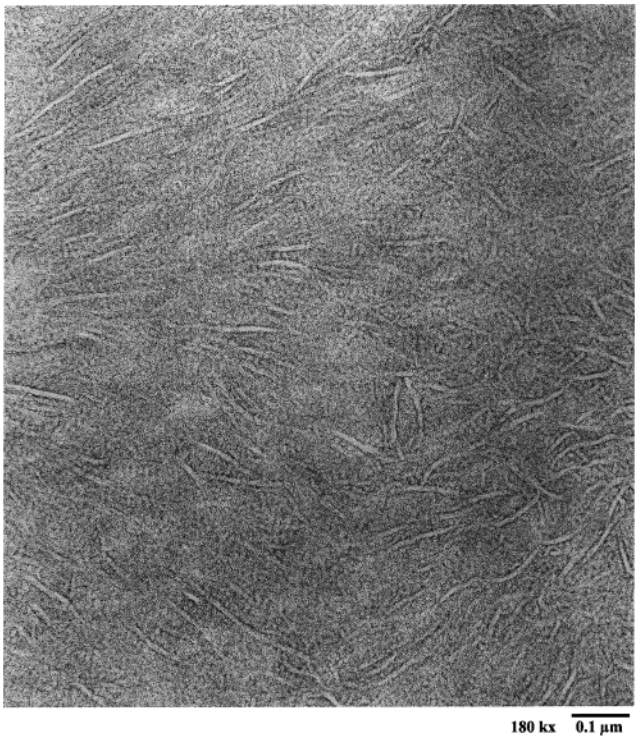

Figure 9. TEM of d-HDPE/HPBD-2 (25/75) blend rapidly quenched from the melt.

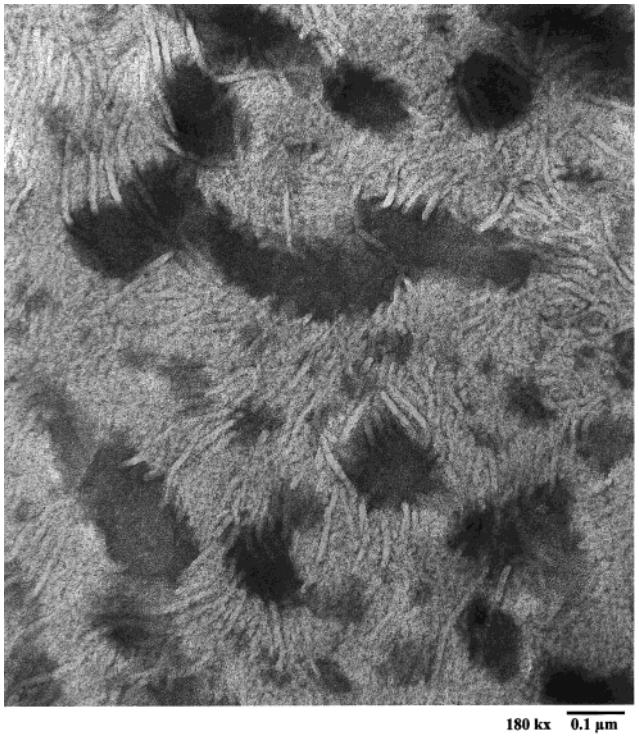

Figure 10. TEM of d-HDPE/HPBD-10 (25/75) blend rapidly quenched. HPBD-10 is a hydrogenated polybutadiene with 10.6 mol % ethyl branches.

branched one in lamellae of ~80 Å thick. These lamellae form the skeleton of a homogeneous spherulitic pattern and are significantly thinner than the ~120 Å thick one formed from quenched pure d-HDPE. The shorter sequences and uncocrystallized HPBD-2 (if any) form the thinner, more segmented lamellae that cover the background morphology of Figure 9. The results from solvent extraction experiments also indicated that the branched component must be cocrystallized with the linear since only <3% of the HPBD-2 was extracted at a temperature above the dissolution temperature of the pure HPBD-2.[13]

The lamellae of Figure 9 must form as a consequence of the difference in crystallization kinetics between the branched and linear polyethylenes. They do not segregate in different scale domains. PE blends that show segregation in a domain scale as a consequence of liquid−liquid phase separation have a very distinctive fingerprint morphology, such as that shown in Figure 10. This figure is a TEM micrograph of a 75/25 blend of the d-HDPE (75%) and a hydrogenated polybutadiene with 10.6 mol % of ethyl branches and $M_w = 77\,800$ g/mol. This blend was also rapidly quenched to −78 °C from the melt. SANS plots of this blend were given in Figures 8 and 9 of Alamo et al.,[2] and indicated phase segregation in the melt. Thus, in Figure 10, discrete domains (>0.1 μm in size) of the branched amorphous component are clearly distinguished from the ~120Å thick lamellae formed from the linear component.

The drastic differences between Figures 9 and 10 document once more that the d-HDPE/HPBD-2 blends crystallized from homogeneous melts. Rapidly quenched blends present a lamellar morphology where the components cocrystallized to a different extent depending on the initial blend composition. The Lorentz-corrected SAXS data [$Q^2 d\Sigma/d\Omega)(Q)$ vs Q] for the rapidly quenched blends are given in Figure 11 and show one peak in agreement with the single lamellar stack morphology

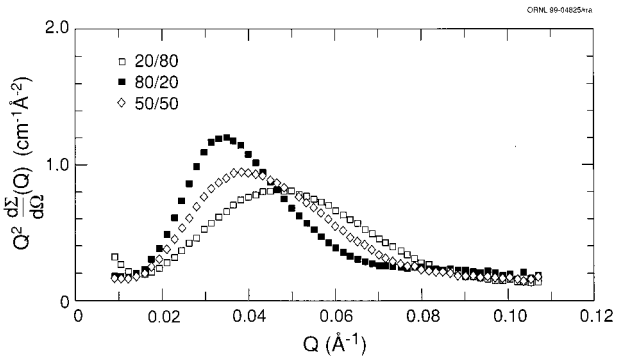

Figure 11. Lorentz-corrected SAXS data for d-HDPE/HPBD-2 blends rapidly quenched from the melt.

shown by these blends. The long periods, calculated from the peak, increase monotonically with increasing concentration of the linear component with values of 131, 138, 162, and 190 Å for the 0/100, 20/80, 50/50, and 80/20 blends of d-HDPE/HDBD-2 blends. The peaks of Figure 11 broaden considerably with increasing concentration of the branched component, indicating an increase in the population of thin lamellar stacks, as shown in Figure 8.

SANS data were also collected on these blends following rapid quenching from the melt. In agreement with the morphology described above, these samples gave qualitatively different SANS patterns to the isothermally crystallized or slow-cooled samples, which vary as Q^{-4} in the high-Q limit (Figure 12), as predicted by eq 1. Figure 13 shows a log−log plot of SANS data from the 20/80 d-HDPE/HPBD-2 sample rapidly quenched from the melt. It may be seen that at high Q the data approach the Q^{-2} asymptote as opposed to the Q^{-4} behavior observed for slowly cooled and isothermally crystallized blends (Figure 12 and eq 1). This suggests that the scattering arises from individual molecules ($d\Sigma$/

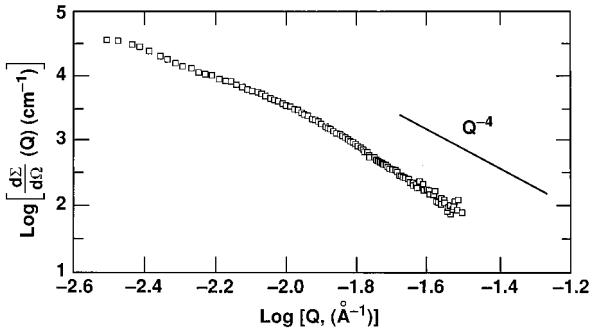

Figure 12. log−log plot for 20/80 d-HDPE/HPBD-2 blend isothermally crystallized at 117 °C.

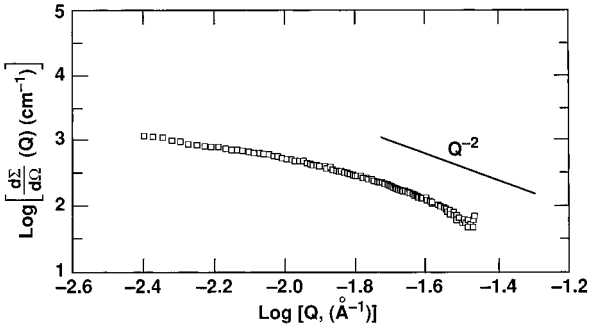

Figure 13. log−log plot for 20/80 d-HDPE/HPBD-2 blend rapidly quenched from the melt.

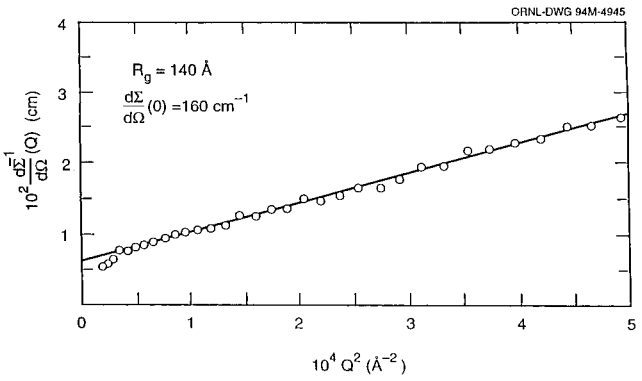

Figure 14. $[(d\Sigma/d\Omega)(Q)]^{-1}$ vs Q^2 for 10/90 sample of d-HDPE/LDPE rapidly quenched to −78 °C. From Wignall et al.[3]

$d\Omega - Q^{-2}$) rather than separate phases with sharp boundaries ($d\Sigma/d\Omega - Q^{-4}$), and similar behavior was observed for rapidly crystallized blends of HDPE/LDPE.[3] Figure 14 shows a Zimm plot [$d\Sigma/d\Omega^{-1}$ (Q) vs Q^2] of the SANS data from a quenched 10/90 HDPE-D/LDPE. The cross section [$d\Sigma/d\Omega(0) = 160$ cm^{-1}] and radius of gyration ($R_g \sim 140$ Å) are similar to the molecular dimensions measured in the solid state for HDPE-D/HDPE-H blends,[3,33−35] indicating that the D-labeled linear polymer is distributed throughout the LDPE matrix (i.e., cocrystallized with the branched molecules in the lamellae and mixed in the amorphous regions).

Figure 15 shows a Zimm plot for a 20/80 d-HDPE/HPBD-2 blend that was rapidly quenched. The plot is also linear, but the extrapolated values of $d\Sigma/d\Omega(0) \simeq 1200$ cm^{-1} are a factor of approximately 3 higher than calculated. This discrepancy arises from a clustering or segregation artifact,[33−39] and it is known that the true cross-section is observed only when the centers of gravity of the labeled molecules are statistically dispersed in the matrix. Any departure from such a

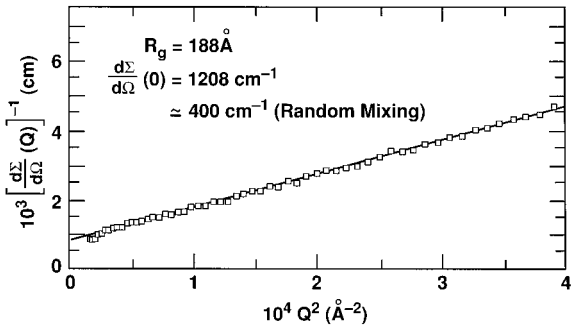

Figure 15. Zimm plot for 20/80 d-HDPE/HPBD-2 blend rapidly quenched from the melt.

distribution either by way of aggregation of the labeled molecules or correlations in their trajectories or positions can lead to excess scattering and hence anomalous values[34,35] of $d\Sigma/d\Omega(0)$ or R_g. Extensive studies of melt-crystallized polyethylene have shown that correlated aggregates of D-labeled molecules are created in the melting region, due to the difference in melting points between the components, which gives rise to differential crystallization effects.[34−38] For rapidly quenched blends of HDPE/LDPE (Figure 14), the molecules do not have sufficient time to rearrange their trajectories substantially, and their centers of gravity remain statistically (randomly) distributed in the solid state.[33−35] However, for the d-HDPE/HPBD-2 system, the HPBD-2 molecules diffuse faster than the LDPE molecules, because they have no long-chain branches. Thus, d-HDPE/HPBD-2 blends will show greater segregation or clustering effects. Conversely, one would expect more cocrystallization in the HDPE/LDPE mixtures, as observed.[3]

Conclusions

A combination of DSC, TEM, SAXS, and SANS techniques have been used to fully characterize the morphology of blends of linear and model linear-low-density polyethylenes crystallized from the melt. SANS indicates that the mixtures are homogeneous in the melt for all compositions when the ethyl branch content in the copolymer is low (i.e., <4 mol % branches). However, when the branch content is higher, the components phase separate in the melt, and this heterogeneous morphology is fixed upon crystallization. A morphology of different domains in the submicron range is clearly observed by TEM of stained sections of these blends. Blends that are homogeneous in the melt may phase segregate in the solid state to different degrees depending on the rate of cooling and the initial composition.

The strongest lamellar segregation is observed for isothermally crystallized blends at temperatures at which the branched component does not crystallize and for the predominantly linear blends. Some mixing of both components is found in the crystals formed on cooling 50/50 blends, and the degree of mixing increases with increasing concentration of the branched component. Segregation in the solid blends is indicated by the double endotherms seen in DSC and the agreement between the experimentally observed and calculated SANS intensity and invariant. SAXS patterns and the lamellae morphology by TEM also confirm this morphology. Slowly cooled blends behave very similarly to the isothermally crystallized ones. However, they show progressively more mixing with increasing concentration of the branched component than their isothermally crystallized counterparts.

The linear component does not segregate in the rapidly crystallized or quenched blends. Instead, cocrystallization of both components takes place, as indicated by single DSC endotherms, by the inability of extracting the branch component at above its dissolution temperature and by SANS intensity fits typical of homogeneous systems. Moreover, Zimm-type plots indicate that some molecular clustering may be present. The SAXS data and TEM micrographs are consistent with those of cocrystallized systems.

Acknowledgment. The research at Oak Ridge was supported by the Division of Materials Sciences, U.S. Department of Energy under Contract No. DE-AC05-840R21400 with Martin Marietta Energy Systems, Inc. The work at Florida State was supported by the National Science Foundation Polymer Program (DMR 94-19508), whose aid is gratefully acknowledged.

References and Notes

(1) Alamo, R. G.; Londono, J. D.; Mandelkern, L.; Stehling, F. C.; Wignall, G. D. *Macromolecules* **1994**, *27*, 411.
(2) Alamo, R. G.; Graessley, W. W.; Krishnamoorti, R.; Lohse, D. J.; Londono, J. D.; Mandelkern, L.; Stehling, F. C.; Wignall, G. D. *Macromolecules* **1997**, *30*, 561.
(3) Wignall, G. D.; Londono, J. D.; Lin, J. S.; Alamo, R. G.; Galante, M. J.; Mandelkern, L. *Macromolecule*s **1995**, *28*, 3156.
(4) Nicholson, J. C.; Finerman, T. M.; Crist, B. *Polymer* **1990**, *31*, 2287.
(5) Norton, D. R.; Keller, A. *J. Mater. Sci.* **1984**, *19*, 447.
(6) Reckinger, C.; Larbi, F. C.; Rault, J. *J. Macromol. Sci., Phys.* **1984**−**1985**, *B23*, 511.
(7) Hu, S.-R.; Kyu, T.; Stein, R. S. *J. Polym. Sci., Polym. Phys. Ed.* **1987**, *25*, 71.
(8) Hill, M. J.; Barham, P. J.; van Ruiten, *J. Polym.* **1993**, *24*, 2975.
(9) Hill, M. J.; Organ, S. J.; Barham, P. J. *Thermochim. Acta* **1994**, *238*, 17.
(10) Crist, B.; Hill, M. J. *J. Polym. Sci., Polym. Phys. Ed.* **1997**, *35*, 2329.
(11) Hill, M. J.; Barham, P. J. *Polymer* **1997**, *38***,** 5595.
(12) Wignall, G. D.; Alamo, R. G.; Londono, J. D.; Mandelkern, L.; Stehling, F. C. *Macromolecules* **1996**, *29*, 9**,** 5332.
(13) Alamo, R. G.; Glazer, R. H.; Mandelkern, L. *J. Polym. Sci., Polym. Phys. Ed.* **1988**, *26*, 2167.
(14) Quinn, F. A., Jr.; Mandelkern, L. *J. Am. Chem. Soc.* **1958**, *80*, 3178.
(15) On the basis of the work of Bates et al.,[16] the heat of fusion, per mole of crystalline repeating unit, of protonated and deuterated polyethylene is taken to be the same. Thus, on a per gram basis, there is approximately 14% difference in ΔH.
(16) Bates, F. S.; Keith, H. D.; McWhan, D. B. *Macromolecules* **1987**, *20*, 3065.
(17) Brown, G. M.; Butler, J. H. *Polymer* **1997**, *38*, 3937.
(18) Morgan, R. L.; Hill, M. J.; Barham, P. J. *Polymer* **1999**, *40*, 337.
(19) Koehler, W. C. *Physica (Utrecht)* **1986**, *137B*, 320.
(20) Wignall, G. D.; Bates, F. S. *J. Appl. Crystallogr.* **1986**, *20*, 28.
(21) Hayashi, H.; Flory, P. J.; Wignall, G. D. *Macromolecules* **1983**, *16*, 1328.
(22) Hendricks, R. W. *J. Appl. Phys.* **1978**, *11*, 15.
(23) Wignall, G. D.; Lin, J. S.; Spooner, S. *J. Appl. Cryst.* **1990**, *23*, 241.
(24) Wignall, G. D. *J. Appl. Crystallogr.* **1991**, *24*, 479.
(25) Russell, T. P.; Lin, J. S.; Spooner, S.; Wignall, G. D. *J. Appl. Cryst.* **1988**, *21*, 629.
(26) Debye, P.; Bueche, A. M. *J. Appl. Phys.* **1949**, *20*, 518.
(27) Debye, P.; Anderson, H. R.; Brumberger, H. *J. Appl. Phys.* **1957**, *28*, 679.
(28) Agamalian, M. M.; Wignall, G. D.; Triolo, R. *J. Appl. Cryst.* **1997**, *30*, 345.
(29) Vonk, C. G. In *Small Angle X-ray Scattering*; Glatter, D., Kratky, O., Eds.; Academic Press: New York, 1982.
(30) Cheung, Y. W.; Stein, R. S.; Lin, J. S.; Wignall, G. D. *Macromolecules*, **1994**, *27*, 2520.
(31) Galante, M. J.; Mandelkern, L.; Alamo, R. G. *Polymer* **1998**, *39*, 5105.
(32) Agamalian, M.; Alamo, R. G.; Kim, M. H.; Londono, J. D.; Mandelkern, L.; Wignall, G. D. *Macromolecules* **1999**, *32*, 3093.
(33) Wignall, G. D.; Ballard, D. G. H.; Schelten, J. *J. Macromol. Sci.* **1976**, *B12*, 99.
(34) Schelten, J.; Wignall, G. D.; Ballard, D. G. H.; Longman, G. W. *Polymer* **1977**, *18*, 111.
(35) Schelten, J.; Wignall, G. D.; Ballard, D. G. H.; Longman, G. W.; Schmatz, W. *Polymer* **1976**, *17*, 751.
(36) Sadler, D. In *The Structure of Crystalline Polymers*; Hall, I., Ed.; Applied Science Publishers: New York, 1983; p 125.
(37) Wignall, G. D.; Wu, W. *Polym. Commun.* **1983**, *24*, 354.
(38) Wu, W.; Wignall, G. D. *Polymer* **1985**, *26*, 661.
(39) Summerfield, G. C.; King, J. S.; Ullman, R. *Macromolecules* **1978**, *11*, 218.

MA9912655